

# CHEMISTRY

## A European Journal

A Journal of



### Accepted Article

**Title:** Light-Controlled Reversible Modulation of Frontier Molecular Orbital Energy Levels in Trifluoromethylated Diarylethenes

**Authors:** Martin Herder, Fabian Eisenreich, Aurelio Bonasera, Anna Graf, Lutz Grubert, Michael Pätzelt, Jutta Schwarz, and Stefan Hecht

This manuscript has been accepted after peer review and appears as an Accepted Article online prior to editing, proofing, and formal publication of the final Version of Record (VoR). This work is currently citable by using the Digital Object Identifier (DOI) given below. The VoR will be published online in Early View as soon as possible and may be different to this Accepted Article as a result of editing. Readers should obtain the VoR from the journal website shown below when it is published to ensure accuracy of information. The authors are responsible for the content of this Accepted Article.

**To be cited as:** *Chem. Eur. J.* 10.1002/chem.201605511

**Link to VoR:** <http://dx.doi.org/10.1002/chem.201605511>

Supported by  
**ACES**

WILEY-VCH

# Light-Controlled Reversible Modulation of Frontier Molecular Orbital Energy Levels in Trifluoromethylated Diarylethenes

Martin Herder, Fabian Eisenreich, Aurelio Bonasera, Anna Grafl, Lutz Grubert, Michael Pätzelt, Jutta Schwarz, and Stefan Hecht<sup>[a]</sup>

**Abstract:** Among bistable photochromic molecules diarylethenes (DAEs) possess the distinct feature that upon photoisomerization they undergo a large modulation of their  $\pi$ -electronic system, accompanied by a marked shift of the HOMO/LUMO energies and hence oxidation/reduction potentials. The electronic modulation can be utilized to remote-control charge as well as energy transfer processes and it can be transduced to functional entities adjacent to the DAE core, thereby regulating their properties. In order to exploit such photoswitchable systems it is important to precisely adjust the absolute position of their HOMO and LUMO levels and to maximize the extent of the photoinduced shifts of these energy levels. Here, we present a comprehensive study detailing how variation of the substitution pattern of DAE compounds, in particular using strongly electron-accepting and chemically stable trifluoromethyl groups either in the periphery or at the reactive carbon atoms, allows for the precise tuning of frontier molecular orbital levels over a broad energy range and the generation of photoinduced shifts of more than 1 eV. Furthermore, the effect of different DAE architectures on the transduction of these shifts to an adjacent functional group is discussed. Whereas substitution in the periphery of the DAE motif has only minor implications on the photochemistry, trifluoromethylation at the reactive carbon atoms strongly disturbs the isomerization efficiency. However, this can be overcome by using a nonsymmetrical substitution pattern or by combination with donor groups, rendering the resulting photoswitches attractive candidates for the construction of remote-controlled functional systems.

## Introduction

Photoswitchable compounds, which can be reversibly interconverted between two (meta)stable isomers by irradiation with light,<sup>[1]</sup> are powerful tools for the design of molecules and materials thereof that exert their function on demand and in a highly controlled fashion. The simplest remote-controllable function of a photochromic molecule is the absorption of light of distinct wavelengths and thus the emergence of color. However, there are more physical and chemical properties of the photochromic moiety that are altered upon isomerization, such

as molecular geometry, dipole moment, and electronic structure, and hence many other functions can be switched on and off by light. Consequently the interest in applying photoswitchable molecules has recently grown in diverse fields ranging from pharmacology<sup>[2]</sup> over molecular machines<sup>[3]</sup> to organic electronics.<sup>[4]</sup>

For the realization of such "smart" systems diarylethenes (DAEs)<sup>[5]</sup> are a highly attractive class of photochromic compounds with a number of properties that render them superior to others: in general, the photochemical interconversion between their open and closed form is very efficient, both isomers are thermally stable, and they can be designed to possess outstanding fatigue resistance. Looking into the literature two principal strategies can be identified how the photochromic reaction of DAEs can be translated into a remote-controllable function:<sup>[6]</sup> Some examples in the areas of photoactuation,<sup>[7]</sup> responsive supramolecular assemblies<sup>[8]</sup> or binding to biological targets<sup>[9]</sup> rely on the modulation of molecular geometry and flexibility of the DAE core upon isomerization, though it is generally small compared to other photoswitchable molecules, such as azobenzenes. The vast majority of applications of DAEs, however, are based on the marked electronic changes occurring upon isomerization with a reorganization of their  $\pi$ -electronic structure accompanied by a significant shift of the energies of their frontier molecular orbitals (Figure 1a).

One way to utilize this feature in order to gain remote-control over a specific function is to implement inter- or intramolecular energy or charge transfer processes between the DAE and a functional moiety, whose efficiency will be different in the two isomeric forms. Exemplarily, the emission of fluorophores attached to DAEs can be quenched by energy or electron transfer typically to the ring-closed isomer with its reduced energy gap.<sup>[10]</sup> Likewise other excited state processes such as singlet oxygen sensitization<sup>[11]</sup> or triplet triplet annihilation<sup>[12]</sup> can be reversibly quenched by DAEs. Another obvious application is the photomodulation of conductance through single DAE molecules<sup>[13]</sup> as well as the charge transport through molecular ensembles within organic electronic devices.<sup>[14]</sup> In recent work we demonstrated that by combining DAEs and high-performing organic semiconductors by a simple blending approach effective photocontrol over charge carrier mobilities in transistors can be achieved and flexible, non-volatile optical memories be realized.<sup>[15]</sup> In these devices, the precise alignment of the HOMO and LUMO levels of the two DAE isomers relative to the ones of the semiconducting host material is the key to induce light-induced reversible charge trapping by the photochromic molecules. Consequently, to further improve these systems we are highly interested in the underlying electronic structure-property relationships of DAEs and want to understand: i) how to

[a] Dr. M. Herder, F. Eisenreich, Dr. A. Bonasera, A. Grafl, Dr. L. Grubert, Dr. M. Pätzelt, J. Schwarz, Prof. Dr. S. Hecht  
Department of Chemistry & IRIS Adlershof  
Humboldt-Universität zu Berlin  
Brook-Taylor-Str. 2, 12489 Berlin (Germany)  
E-mail: sh@chemie.hu-berlin.de

Supporting information for this article is given via a link at the end of the document

precisely engineer the *absolute* energetic positioning of the HOMO/LUMO levels of the isomers and ii) how to maximize the *relative* shifts in HOMO/LUMO energies upon isomerization.

In our previous work we found that introduction of chemically inert trifluoromethyl ( $\text{CF}_3$ ) groups is particularly attractive: Either in the periphery of the DAE structure at the terminal phenyl groups, where they significantly improve the fatigue resistance of the switching process,<sup>[16]</sup> or as a replacement of the methyl groups in reactive  $\alpha$ -position of the hetaryl rings, where a huge impact on the oxidation and reduction potentials was observed.<sup>[17]</sup> To obtain a more systematic insight on the impact of trifluoromethyl substitution on the photochemistry and in particular on the electronic properties of DAEs, we now prepared a set of model compounds possessing  $\text{CF}_3$  groups either in the periphery or in the  $\alpha$ -position within thiophene and thiazole series and compared these with standard DAE derivatives possessing electron neutral or donor groups (Figure 1b).

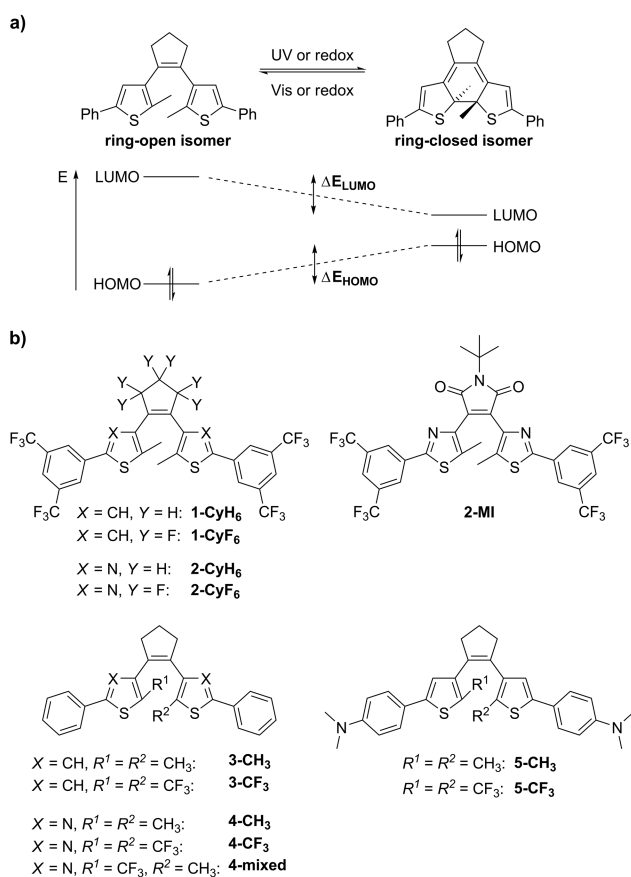


**Figure 1.** a) Modulation of DAE core HOMO/LUMO levels upon light (or redox) induced isomerization. b) Trifluoromethylated DAE derivatives for investigating the extent of their HOMO/LUMO level modulation.

Besides relying on charge (or energy) transfer processes another strategy to remote-control functions is to transduce electronic changes occurring within the DAE core to an adjacent functional group, such as a reactive group, a catalyst or a supramolecular binding motif. Thereby, the reshuffling of double bonds upon the isomerization reaction allows for the reversible electronic coupling of the functional group with donor or acceptor groups, thus modulating its electron density and hence acidity/basicity and/or electrophilicity/nucleophilicity. In principle, several strategies involving three different architectures with distinct  $\pi$ -conjugation pathways are conceivable (Figure 2). In many cases the functional unit serves as the bridge of the DAE scaffold, thus its properties are modulated upon ring-closure by turning the central double bond into a single bond and by bringing donor or acceptor groups attached to the hetaryl rings into conjugation to the bridge (Figure 2a). Alternatively, the functional unit can be placed in the periphery of the DAE, for example as substituent of one hetaryl ring (Figure 2b). The isomerization reaction effects a coupling/decoupling with donor or acceptor groups, placed either on the opposite hetaryl ring or in the opposite  $\alpha$ -position of the same hetaryl ring. For all three architectures examples of DAEs modulating the properties of a functional unit can be found in the literature.<sup>[18]</sup> However, a direct comparison to evaluate which structure provides the largest transduction of electronic effects to a given functional unit upon switching is difficult.

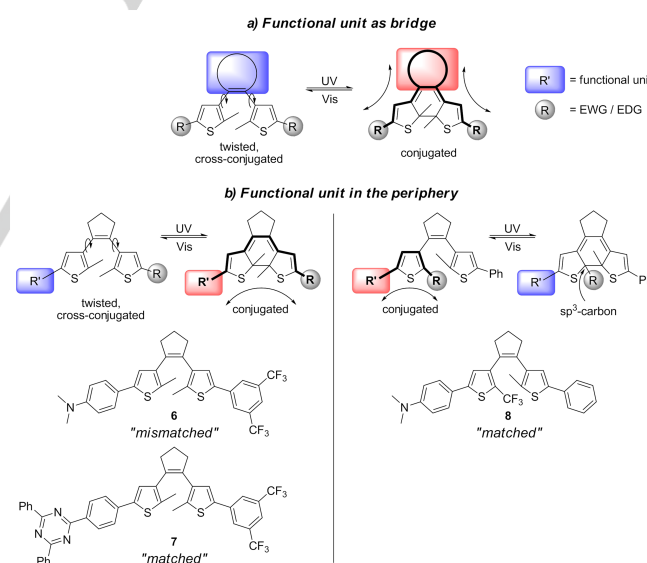


**Figure 2.** Structural approaches for transducing the photoinduced electronic changes of DAEs to an attached functional group by coupling/decoupling it with electron-donating/-withdrawing groups (EDG/EWG): a) Incorporation of the functional unit as the bridge. b) Attachment of the functional unit in the periphery using donor/acceptor substituents either on the opposite (left) or the same (right) thiophene ring. Below DAEs with redox active *N,N*-dimethylaniline and triphenyltriazine moieties and differently placed trifluoromethyl groups to evaluate their effect are shown.

To address this question, model compounds **6-8** were designed bearing redox active *N,N*-dimethylaminophenyl or triphenyltriazine moieties in the periphery and the changes in their oxidation or reduction potential, respectively, occurring upon photoisomerization were monitored. Trifluoromethyl groups were chosen as acceptor moieties, either in the form of 3,5-bis(trifluoromethyl)phenyl substituents (**6** and **7**) or directly attached to the  $\alpha$ -position of the thiophene ring (**8**). Compound **6** can be regarded as a "mismatched" case since two effects are opposing each other: The  $\pi$ -system of the DAE becomes extended during the course of cyclization, leading to a decrease of the amine's oxidation potential in the closed isomer, whereas the established electronic coupling between the amine and the acceptor group on the other thiophene ring should increase the amine's oxidation potential. In contrast, compounds **7** and **8** resemble "matched" cases, for which the change in conjugation and coupling/decoupling of the acceptor units cooperate, *i.e.* lowering the oxidation or reduction potentials of the amine or triazine, respectively, upon ring-closure. Thus, for model DAEs **7** and **8** more pronounced potential differences between the isomers are expected. Note that the bridge-functionalized architecture has already been investigated by us in a previous study.<sup>[19]</sup> The reduction potential of a bridging maleimide "matched" with acceptor substituents in the periphery was reduced by 240 mV upon ring-closure, while the "mismatched" derivative bearing donor groups showed a change of only 70 mV. This electronic difference was directly related to a difference in the function of the maleimide, *i.e.* the strength of the binding to a receptor via hydrogen-bonding interactions.

Here, we report on the synthesis and the photochemistry as well as the redox properties of various types of trifluoromethylated DAEs. We discuss the implications of the different substitution patterns on the absolute position of the frontier molecular orbital energy levels and their relative photoinduced shifts. Furthermore, we analyze the interplay of substituent and conjugation effects in "matched" and "mismatched" DAE architectures to uncover the optimal strategy for achieving maximum electronic changes upon photoswitching.

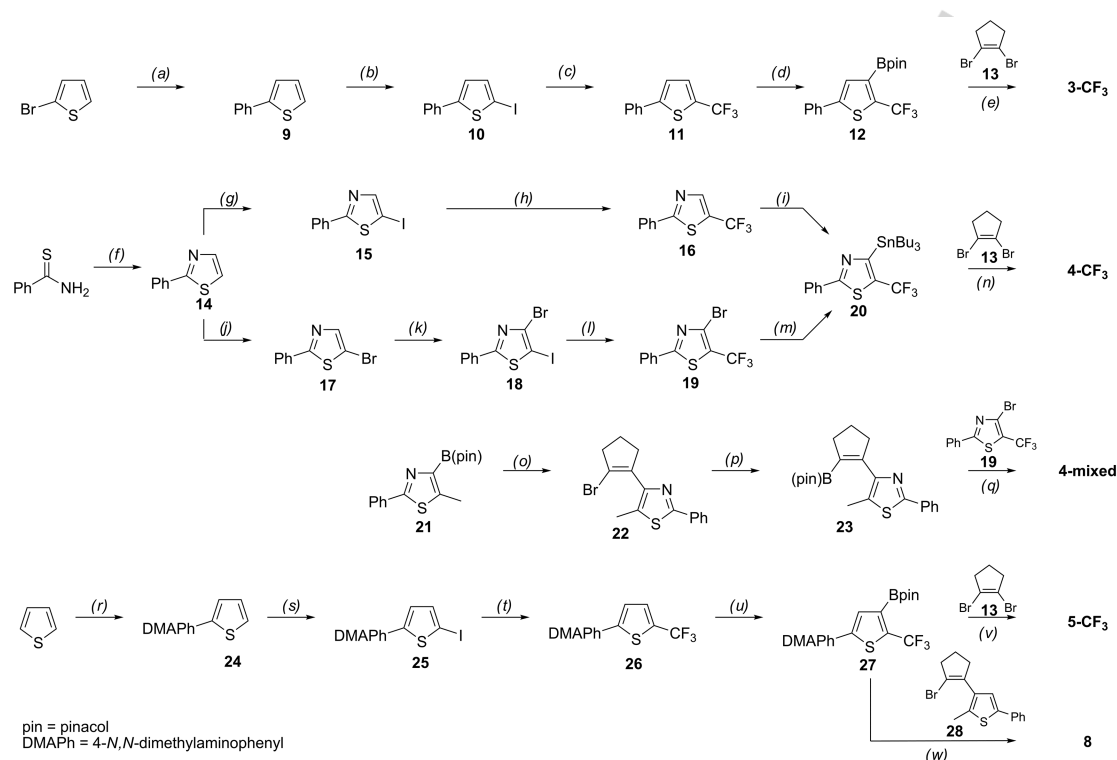
## Results and Discussion

**Synthesis.** The syntheses of DAEs **1-CyH<sub>6</sub>**, **1-CyF<sub>6</sub>**, **2-CyH<sub>6</sub>**, **2-CyF<sub>6</sub>**, **3-CH<sub>3</sub>**, **4-CH<sub>3</sub>**, **5-CH<sub>3</sub>**, and **6** were reported by us previously<sup>[16]</sup> and followed the established strategies of cross-coupling of pre-functionalized thiophene or thiazole building blocks with the respective dihalogenated bridging units<sup>[20]</sup> or the (stepwise) functionalization of the 1,2-bis(2-chloro-5-methylthien-4-yl)cyclopentene building block.<sup>[21]</sup> Details for the analogous synthesis of DAEs **2-MI** and **7** can be found in the Supporting Information.

For the synthesis of  $\alpha$ -CF<sub>3</sub> substituted DAEs the heterocycles were pre-assembled with the key step being the trifluoromethylation of the thiophene or thiazole rings (Scheme 1). In case of the thiophene derivatives, trifluoromethylation was achieved in moderate yields following a procedure by Urata and Fuchikami<sup>[22]</sup> consisting of reacting 2-

iodo-5-phenylthiophene **10** or 2-iodo-5-(4-*N,N*-dimethylaminophenyl)thiophene **25** with TMSCF<sub>3</sub> in presence of stoichiometric amounts of CuI and KF. Due to the electron withdrawing nature of the CF<sub>3</sub> group the resulting  $\alpha$ -trifluoromethylated thiophenes **11** and **26** could easily be metalated in the adjacent  $\beta$ -position using LDA and transformed into their pinacolboronic esters, which finally were cross-coupled with 1,2-dibromocyclopentene **13** or the already monofunctionalized analogue **28** to afford DAEs **3-CF<sub>3</sub>**, **5-CF<sub>3</sub>**, and **6**, respectively.

In the thiazole series, 5-iodo-2-phenylthiazole **15** could be trifluoromethylated in yields superior to that of Urata and Fuchikami's method using the *in-situ* generation of Hartwig's "trifluoromethylator" [(phen)CuCF<sub>3</sub>] (phen = phenanthroline).<sup>[23]</sup> However, attempts to increase the scale of the reaction from the suggested 0.5 mmol scale drastically decreased the yield in our hands. The resulting  $\alpha$ -CF<sub>3</sub> thiazole **16** could be metalated using LDA and transformed into its organostannane **20** in only moderate yield due to partial decomposition. To improve the metalation step a bromine substituent was introduced in the 4-position of the thiazole via 5-bromo-2-phenylthiazole **17**, which reacted in a halogen-dance-reaction<sup>[24]</sup> to 4-bromo-5-iodo-2-phenylthiazole **18** and was then trifluoromethylated in the 5-position using the [(phen)CuCF<sub>3</sub>] complex with excellent selectivity. The resulting 4-bromo-2-phenyl-5-trifluoromethylthiazole **19** could subsequently be lithiated at very low temperatures (-100 °C) and transformed into the organostannane **20**, which however had again to be purified by column chromatography lowering the yield. Finally, cross-coupling of the organostannane **20** with 1,2-dibromocyclopentene **13** gave DAE **4-CF<sub>3</sub>**, while the reaction of an already monofunctionalized bromocyclopentene **22** with 4-bromo-2-phenyl-5-trifluoromethylthiazole **19** gave the nonsymmetrically substituted analogue **4-mixed**.



**Scheme 1.** Synthesis of  $\alpha$ -trifluoromethylated diarylethenes: (a)  $\text{PhB}(\text{OH})_2$ ,  $\text{Pd}(\text{PPh}_3)_4$ ,  $\text{Na}_2\text{CO}_3$ , toluene, 100 °C, 16 h, 99%; (b)  $\text{NaI}$ ,  $\text{NCS}$ ,  $\text{AcOH}$ , rt, 3 d, 81%; (c)  $\text{TMSCF}_3$ ,  $\text{CuI}$ ,  $\text{KF}$ ,  $\text{DMF/NMP}$  1:1, 50 °C, 24 h, 49%; (d) 1)  $\text{LDA}$ ,  $\text{THF}$ , -78 °C, 10 min, 2) (*i*-PrO)Bpin, -78 °C to rt, 2 h, quant.; (e) 1,2-dibromocyclopentene **13**,  $\text{Pd}(\text{OAc})_2$ ,  $\text{SPhos}$ ,  $\text{K}_3\text{PO}_4$ , toluene, 100 °C, 24 h, 46%; (f) 2-bromoacetaldehyde diethylacetal, *p*-TsOH,  $\text{EtOH}/\text{H}_2\text{O}$ , 100 °C, 16 h, 97%; (g) 1) *n*-BuLi,  $\text{THF}$ , -80 °C to -10 °C, 30 min, 2)  $\text{I}_2$ , -10 °C, 30 min, 82%; (h)  $\text{TMSCF}_3$ ,  $\text{CuCl}$ ,  $\text{KOtBu}$ , phenanthroline,  $\text{DMF}$ , 50 °C, 18 h, 77%; (i) 1)  $\text{LDA}$ ,  $\text{THF}$ , -78 °C, 45 min, 2)  $\text{Bu}_3\text{SnCl}$ , -78 °C, 15 min, 68%; (j)  $\text{Br}_2$ ,  $\text{AcOH}$ , rt, 16 h, 64%; (k) 1)  $\text{LDA}$ ,  $\text{THF}$ , -78 °C, 30 min, 2)  $\text{I}_2$ , -78 °C, 30 min, 92%; (l)  $\text{TMSCF}_3$ ,  $\text{CuCl}$ ,  $\text{KOtBu}$ , phenanthroline,  $\text{DMF}$ , 50 °C, 18 h, 80%; (m) 1) *n*-BuLi,  $\text{THF}$ , -100 °C, 45 min, 2)  $\text{Bu}_3\text{SnCl}$ , -85 °C, 30 min; (n) 1,2-dibromocyclopentene **13**,  $\text{PdCl}_2(\text{PPh}_3)_2$ ,  $\text{DMF}$ , 100 °C, 18 h, 18%; (o)  $\text{Pd}(\text{OAc})_2$ ,  $\text{SPhos}$ ,  $\text{K}_3\text{PO}_4$ , toluene, 100 °C, 16 h, 61%; (p) 1) *n*-BuLi,  $\text{THF}$ , -78 °C, 45 min, 2) (*i*-PrO)Bpin, -78 °C to rt, 16 h, quant.; (q) **19**,  $\text{Pd}(\text{OAc})_2$ ,  $\text{Cs}_2\text{CO}_3$ ,  $\text{DavePhos}$ ,  $\text{EtOH}/\text{THF}/\text{DMF}$  4:4:1, 70 °C, 16 h, 43%; (r) 1) *n*-BuLi,  $\text{THF}$ , -78 °C, 1 h, 2)  $\text{B}(\text{O}i\text{Bu})_3$ , -78 °C to rt, 1 h, 3) 4-bromo-*N,N*-dimethylaniline,  $\text{PdCl}_2(\text{dppf})$ ,  $\text{Na}_2\text{CO}_3$ ,  $\text{THF}/\text{EtOH}$ , 75 °C, 4 h, 79%; (s) 1) *n*-BuLi,  $\text{THF}$ , -60 °C, 45 min, 2)  $\text{I}_2$ , -60 °C to rt, 20 min, 78%; (t)  $\text{TMSCF}_3$ ,  $\text{CuI}$ ,  $\text{KF}$ ,  $\text{DMF/NMP}$  1:1, 55 °C, 16 h, 69%; (u) 1)  $\text{LDA}$ ,  $\text{THF}$ , -78 °C, 30 min, 2) (*i*-PrO)Bpin, -78 °C to rt, 30 min, quant. (v) 1,2-dibromocyclopentene **13**,  $\text{PdCl}_2(\text{dppf})$ ,  $\text{K}_3\text{PO}_4$ , dioxane, 100 °C, 18 h, 27%; (w) **28**,  $\text{Pd}(\text{OAc})_2$ ,  $\text{SPhos}$ , toluene, 100 °C, 20 h, 56%.

**Photochemistry.** The photochemical properties of  $\alpha$ -methyl functionalized DAEs **1-CyH<sub>6</sub>**, **1-CyF<sub>6</sub>**, **2-CyH<sub>6</sub>**, **2-CyF<sub>6</sub>**, **3-CH<sub>3</sub>**, **4-CH<sub>3</sub>**, **5-CH<sub>3</sub>**, and **6** were previously described in detail<sup>[16]</sup> and are summarized in Table 1. They generally show an efficient ring-closure upon UV irradiation with quantum yields  $\Phi_{AB}$  in the range 0.4 – 0.7, whereas quantum yields for ring-opening upon visible light irradiation  $\Phi_{BA}$  are more than one order of magnitude smaller. This ensures high conversions to the ring-closed isomer in the photostationary state (PSS) reached upon UV irradiation, generally exceeding 90%, though both isomers absorb UV light. Only derivative **6** possessing a strong donor and acceptor substituent on either side of the DAE structure represents a marked exception with its quantum yields in both isomerization directions being smaller by one order of magnitude when compared to the symmetrically donor or acceptor substituted analogues **5-CH<sub>3</sub>** and **1-CyH<sub>6</sub>**, respectively.

Compounds **2-MI** and **7** also show the expected behavior for  $\alpha$ -methyl functionalized DAEs with small deviations resulting from the substituents. In UV/vis spectra (see section 1.2 of the

Supporting Information) the ring-open isomer of **2-MI** shows a weak, broad charge transfer (CT) band extending to the visible range besides the strong  $\pi$ - $\pi^*$  transition, which is a typical property of DAEs substituted with the strongly electron-withdrawing maleimide bridge.<sup>[17,19,25]</sup> Potentially due to the competing CT process the quantum yield for ring-closure is somewhat smaller than for the corresponding (perfluoro)cyclopentene-bridged DAEs. However, in contrast to analogous dithiazolymaleimides bearing strong donor substituents on the thiazole rings,<sup>[17]</sup> cyclization of **2-MI** is still possible with a reasonable efficiency. For DAE **7**, a bathochromically shifted absorbance is observed of both the open and closed isomers as compared to that of prototype DAE **1-CyH<sub>6</sub>**, reflecting the extension of the  $\pi$ -system by the triphenyltriazine moiety. While ring-closure of **7** is associated with a high quantum yield  $\Phi_{AB} = 0.62$ , the reverse ring-opening process is much less efficient when compared to **1-CyH<sub>6</sub>**, presumably due to stabilization of the closed isomer by the elongated  $\pi$ -system.<sup>[26]</sup>



**Table 1.** Photophysical properties of investigated diarylethenes in acetonitrile (25 °C).

| comp.                                    | $\lambda_{max}$ / nm ( $\epsilon / 10^4 \text{ M}^{-1} \text{ cm}^{-1}$ ) |               | PSS ( $\lambda_{irr}$ ) <sup>[a]</sup> | $\Phi_{AB}$ ( $\lambda_{irr}$ ) <sup>[b]</sup> | $\Phi_{BA}$ ( $\lambda_{irr}$ ) <sup>[c]</sup> |
|--|---|---------------|--|--|--|
|  | open isomer   | closed isomer |  |  |  |
| <b>1-CyH<sub>6</sub></b> <sup>[16]</sup> | 284 (3.16)  | 548 (1.96)    | 97% (313 nm)                           | 0.44 (313 nm)                                  | 0.0046 (546 nm)                                |
| <b>1-CyF<sub>6</sub></b> <sup>[16]</sup> | 300 (3.45)  | 590 (1.54)    | 96% (313 nm)                           | 0.58 (313 nm)                                  | 0.017 (546 nm)                                 |
| <b>2-CyH<sub>6</sub></b> <sup>[16]</sup> | 332 (1.80)  | 522 (1.34)    | 95% (313 nm)                           | 0.56 (313 nm)                                  | 0.015 (546 nm)                                 |
| <b>2-CyF<sub>6</sub></b> <sup>[16]</sup> | 307 (3.11)  | 538 (1.13)    | 89% (313 nm)                           | 0.45 (313 nm)                                  | 0.039 (546 nm)                                 |
| <b>2-MI</b>                              | 310 (2.60),<br>376 (0.44, shoulder)                                       | 532 (1.10)    | 78% (313 nm)                           | 0.14 (313 nm)                                  | 0.031 (546 nm)                                 |
| <b>3-CH<sub>3</sub></b> <sup>[16]</sup>  | 278 (3.25)  | 520 (1.78)    | 98% (313 nm)                           | 0.47 (313 nm)                                  | 0.0093 (546 nm)                                |
| <b>3-CF<sub>3</sub></b>                  | 284 (3.31)  | 493 (2.01)    | 63% (300 nm)                           | 0.061 (300 nm)                                 | 0.076 (546 nm)                                 |
| <b>4-CH<sub>3</sub></b> <sup>[16]</sup>  | 316 (2.13)  | 500 (1.55)    | 94% (313 nm)                           | 0.53 (313 nm)                                  | 0.021 (546 nm)                                 |
| <b>4-CF<sub>3</sub></b>                  | 283 (2.53)  | 469 (1.72)    | 38% (280 nm)<br>39% (300 nm)           | 0.067 (300 nm)                                 | 0.11 (436 nm)                                  |
| <b>4-mixed</b>                           | 292 (2.33)  | 482 (1.67)    | 84% (300 nm)                           | 0.17 (300 nm)                                  | 0.013 (436 nm)                                 |
| <b>5-CH<sub>3</sub></b> <sup>[16]</sup>  | 331 (4.33)  | 537 (2.66)    | 99% (313 nm)                           | 0.74 (313 nm)                                  | 0.0029 (546 nm)                                |
| <b>5-CF<sub>3</sub></b>                  | 345 (4.02)  | 528 (4.05)    | 98% (350 nm)                           | 0.51 (313 nm)<br>0.58 (365 nm)                 | 0.011 (546 nm)                                 |
| <b>6</b> <sup>[16]</sup>                 | 326 (3.37)  | 570 (2.54)    | 97% (313 nm)                           | 0.051 (313 nm)                                 | 0.0022 (546 nm)                                |
| <b>7</b>                                 | 269 (6.27),<br>358 (3.28)   | 568 (2.63)    | 97% (313 nm)                           | 0.62 (313 nm)                                  | 0.0023 (546 nm)                                |
| <b>8</b>                                 | 311 (2.42),<br>346 (2.10)   | 522 (2.80)    | 98% (313 nm)                           | 0.77 (313 nm)                                  | 0.011 (546 nm)                                 |

[a] Amount of closed isomer in the PSS reached after UV irradiation, determined by UPLC. [b] Quantum yields for ring-closure, obtained by evaluation of kinetic traces using ferrioxalate actinometry. [c] Quantum yields for ring-opening, obtained by the initial slope method using Aberchrome 670 actinometry ( $\lambda_{irr} = 546 \text{ nm}$ ) or ferrioxalate actinometry ( $\lambda_{irr} = 436 \text{ nm}$ ).

While the presence of CF<sub>3</sub> groups in the periphery of the DAE structure does not alter the photochemical isomerization between open and closed isomers, their introduction in the  $\alpha$ -position of the heterocycles has dramatic effects. Compared to the parent dithiazolycyclopentene **4-CH<sub>3</sub>**, the doubly  $\alpha$ -trifluoromethylated analogue **4-CF<sub>3</sub>** shows marked hypsochromic shifts of the lowest energy absorption bands in both the open and closed isomer (Figure 1a, see section 1.2 of the Supporting Information). Remarkably, the quantum yield for ring-closure is decreased by almost one order of magnitude to  $\Phi_{AB} = 0.067$  while at the same time the quantum yield for ring-opening  $\Phi_{BA} = 0.11$  is significantly higher when compared to **4-CH<sub>3</sub>**. The rate-increasing effect of  $\alpha$ -CF<sub>3</sub> groups on ring-opening was already observed for maleimide-bridged dithiazolylenes<sup>[17]</sup> and may be due to a general destabilization of the closed isomer by strongly electron-withdrawing groups attached to the reactive carbon atoms.<sup>[27]</sup> Since for **4-CF<sub>3</sub>** the ratio of quantum yields for ring-opening and ring-closure is less favorable the population of the closed isomer in the PSS upon UV illumination is only 39%,

rendering the doubly CF<sub>3</sub> substituted compound a rather inefficient DAE photoswitch.

In order to investigate whether the usual DAE photochemistry can be restored upon replacing only one of the  $\alpha$ -CH<sub>3</sub> groups by an  $\alpha$ -CF<sub>3</sub> group, the nonsymmetrically substituted derivative **4-mixed** was synthesized. In fact, the photochemical characteristics of **4-mixed** are somewhere in between those of the two symmetrical compounds **4-CH<sub>3</sub>** and **4-CF<sub>3</sub>**: The hypsochromic shift of the absorbance is smaller than for **4-CF<sub>3</sub>** (Figure 3a), the decrease of  $\Phi_{AB}$  to a value of 0.17 is less pronounced, ring-opening is as efficient as for **4-CH<sub>3</sub>**, and the amount of the ring-closed isomer in the PSS of 84% is reasonable. Importantly, these results show that an  $\alpha$ -CF<sub>3</sub> group and its strong influence on the electronic properties of the DAE scaffold (*vide infra*) may be utilized at least on one of the heterocyclic building blocks without disturbing the efficiency of photoisomerization too much.

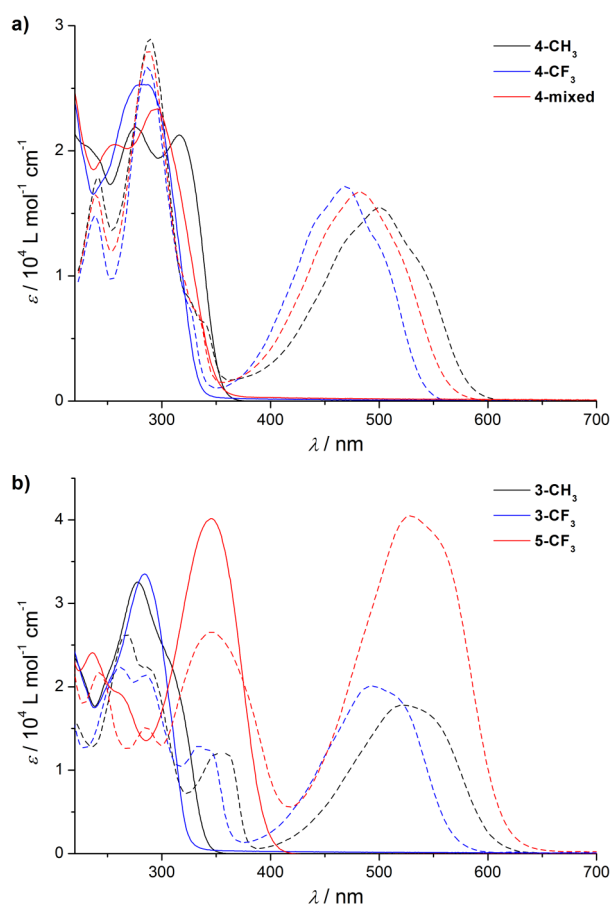


**Figure 3.** Impact of  $\text{CF}_3$  substitution on UV/vis spectra of a) dithiazolyethenes **4-CH<sub>3</sub>**, **4-CF<sub>3</sub>**, and **4-mixed** and b) dithienylethenes **3-CH<sub>3</sub>**, **3-CF<sub>3</sub>**, and **5-CF<sub>3</sub>**. Solid lines represent spectra of pure open isomers in acetonitrile (25 °C), dashed lines represent spectra of the pure closed isomers as calculated from a series of measured spectra at different stages of the irradiation for which the photoconversion was determined by UPLC.

For the thiophene containing DAEs we observed similar trends for  $\alpha\text{-CF}_3$  substitution by comparing compounds **3-CH<sub>3</sub>** and **3-CF<sub>3</sub>** (Figure 3b). Again, replacing both methyl groups by  $\text{CF}_3$  imparts a hypsochromic shift of the absorption bands, a marked decrease of the quantum yield for ring closure, an increased quantum yield for ring-opening, and consequently a reduced amount of the ring-closed isomer in the PSS. Surprisingly, when strongly donating *N,N*-dimethylamino groups are attached to the phenyl rings in combination with  $\alpha\text{-CF}_3$  groups in the symmetrical DAE **5-CF<sub>3</sub>** as well as the nonsymmetrically substituted DAE **8** the typical photochemical behavior is retained. In fact, both show highly efficient ring-closure with quantum yields  $\Phi_{AB} = 0.58$  and  $\Phi_{AB} = 0.77$ , respectively, and almost quantitative conversion to the closed isomer in the PSS.

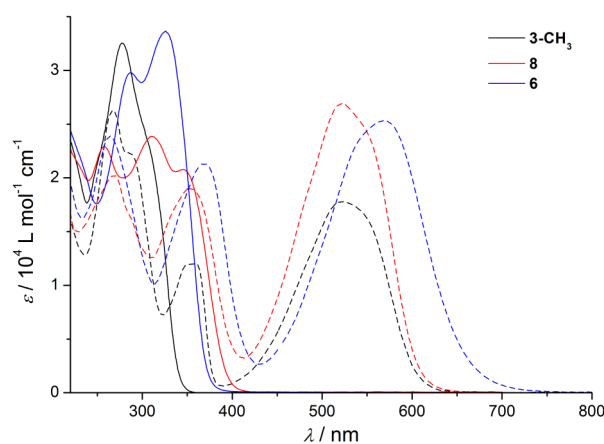


**Figure 4.** Comparison of UV/vis spectra of **3-CH<sub>3</sub>**, **6**, and **8** showing the differing conjugation patterns between donor and acceptor groups. Solid lines represent spectra of pure open isomers in acetonitrile (25 °C), dashed lines represent calculated spectra of the pure closed isomers as calculated from a series of measured spectra at different stages of the irradiation for which the photoconversion was determined by UPLC.

The reason for the severe loss of photocyclization efficiency in case of  $\alpha\text{-CF}_3$  substitution on the hetaryl rings and its recovery upon addition of strongly donating 4-*N,N*-dimethylamino groups to the peripheral phenyl rings remains unclear. It may be due to a change in the relative stabilities of photoreactive and inactive ground state conformations of the ring-open isomer<sup>[28]</sup> or due to an alternating electronic structure leading to the population of excited states with unfavorable orbital topologies for ring-closure.<sup>[29]</sup> Notably, despite the pronounced donor-acceptor substitution of the thiophene rings in DAEs **5-CF<sub>3</sub>** and **8** photocyclization in polar solvents is not prevented by the formation of a twisted intramolecular charge transfer (TICT) state, as it is the case for DAEs bearing electron deficient bridges in combination with electron rich hetaryl rings.<sup>[17,30]</sup>

Comparison of the UV/vis spectra of the prototype DAE **3-CH<sub>3</sub>** with that of the model compounds **6** and **8** (Figure 4) reveals the different conjugation paths between the aniline as a "functional unit" and the acceptor moieties, as claimed in Figure 2. The open form of DAE **8**, with the donor and the acceptor being electronically coupled, shows the most bathochromically shifted absorbance of the investigated open isomers. However, in the closed form the position of the absorbance band in the visible range is almost identical to that of unsubstituted **3-CH<sub>3</sub>**. This shows that the  $\text{CF}_3$  group is efficiently decoupled from the  $\pi$ -system. In contrast, the absorbance of the closed isomer of **6** is shifted bathochromically by 50 nm, revealing the electronic coupling of the donor and the acceptor after ring-closure.

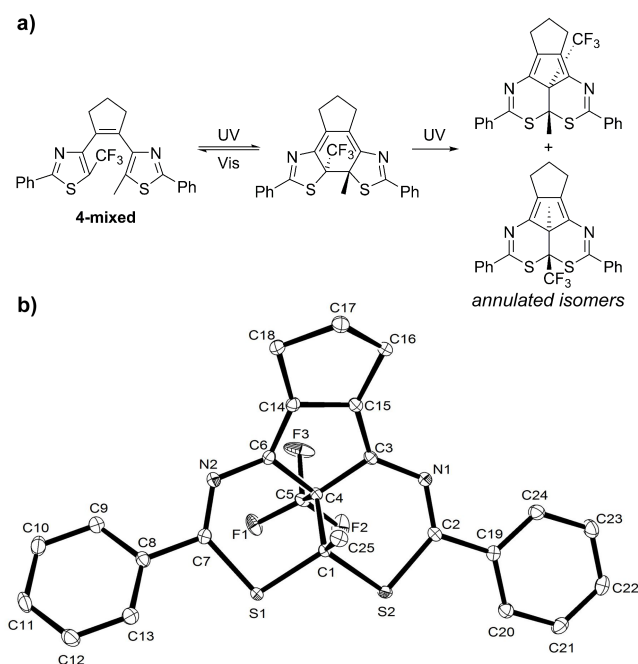


**Figure 5.** a) Formation of two annulated isomers differing in the relative positioning of the CH<sub>3</sub> and CF<sub>3</sub> groups as by-products of the photochemical isomerization of **4-mixed**. b) ORTEP-drawing (50 % probability thermal ellipsoids) of the molecular structure of the isolated annulated isomer of **4-mixed** in the single crystal as determined by X-ray diffraction. Hydrogen atoms and co-crystallized solvent (benzene) are omitted for clarity.

Besides having a strong impact on absorbance spectra and isomerization quantum yields trifluoromethyl substitution of DAEs also alters their photochemical fatigue behavior. As reported earlier,<sup>[16]</sup> substitution with 3,5-bis(trifluoromethyl)phenyl groups in the periphery strongly suppresses the formation of an annulated isomer<sup>[31]</sup> as a by-product of the UV induced cyclization reaction. In contrast, DAEs bearing  $\alpha$ -CF<sub>3</sub> groups exhibit significant fatigue upon repeated switching between the open and closed isomers (see section 1.3 of the Supporting Information). Qualitatively, the switching cycles of  $\alpha$ -trifluoromethylated DAEs **3-CF<sub>3</sub>**, **4-CF<sub>3</sub>**, and **4-mixed** as compared to their methylated analogues **3-CH<sub>3</sub>** and **4-CH<sub>3</sub>** reveal a rather similar overall performance independent of the nature of the group in the  $\alpha$ -position. However, by inspecting UV/Vis spectra and following the switching experiments with UPLC/MS we noted that for DAEs bearing  $\alpha$ -CF<sub>3</sub> groups on both hetaryl rings (**3-CF<sub>3</sub>**, **4-CF<sub>3</sub>**, **5-CF<sub>3</sub>**) the fatigue is not due to the typical selective formation of the annulated isomer but due to the slow decomposition of the DAEs to several yet unidentified photoproducts (see Section 1.3 of the Supporting Information for details). Interestingly, if only one  $\alpha$ -CF<sub>3</sub> group is present (**4-mixed**) two annulated regioisomers, which differ in the positioning of the *anti*-configured methyl and trifluoromethyl groups, are formed in a 1:1 ratio as the only by-products upon prolonged UV irradiation (Figure 5a, Figure S11a). We could isolate one of these annulated isomers and determine its structure by NMR spectroscopy (Figures S12-S13) and X-ray

crystallography (Figure 5b).<sup>[32]</sup> Note that the other isomer detected by UPLC/MS possesses an almost identical absorbance spectrum and the same *m/z* ratio (Figure S11b). The fact that there is no strong preference for one of these annulated isomers may be of importance for the theoretical elucidation of the mechanism of by-product formation. To the present either the cleavage of one C-S bond or the transformation of the central cyclohexadiene core into a methylcyclopentene diradical like structure are discussed as the initial fatigue reaction coordinate in the excited state (Scheme S1).<sup>[33]</sup> However, when molecular symmetry is broken as in **4-mixed**, for both mechanisms a preference for one of the two possible annulated isomers due to the destabilization of intermediate radical species by the CF<sub>3</sub> group could be expected. Thus our experimental finding hints to a more concerted mechanism of the formal type I dyotropic rearrangement as it is considered for other thermally activated reactions of this kind.<sup>[34]</sup>

Remarkably, if the DAE is substituted with a strong donor in the periphery, which generally leads to a poor fatigue resistance,<sup>[16]</sup> attachment of  $\alpha$ -CF<sub>3</sub> groups may lead to a significant improvement. While **5-CH<sub>3</sub>** is one of the DAEs with the worst fatigue resistance in our hands its analogue **5-CF<sub>3</sub>** shows only little decomposition after 11 switching cycles (see Figure S10 in the Supporting Information). Together with the excellent efficiency of the photochromic isomerization and the bathochromically shifted absorbance of the open isomer (*vide supra*) this renders the combination of *N,N*-dimethylaminophenyl and  $\alpha$ -CF<sub>3</sub> groups as hetaryl substituents an interesting motif for the construction of DAEs.

**Modulation of HOMO and LUMO energies.** In this work HOMO and LUMO energy levels of DAE derivatives are calculated from the first oxidation and reduction potentials  $E_p^{a1}$  and  $E_p^{c1}$ , determined by cyclic voltammetry in acetonitrile, according to the following equation ( $e$  = elementary charge):

$$E_{\text{HOMO/LUMO}} = -e \cdot E_p^{a1/c1} - 4.8 \text{ eV} \quad (1)$$

The offset of 4.8 eV represents the ionization potential of ferrocene on the vacuum scale as postulated by Pommerehne and coworkers.<sup>[35]</sup> It is important to note that the utilization of redox potentials as a measure for absolute and relative frontier orbital energies is a rough estimate due to a number of reasons.<sup>[36]</sup>

1) Formally, electrochemistry is not able to directly measure MO levels of a neutral molecule as in the moment an electron is removed or introduced a new species evolves with an altered electronic structure. Furthermore, while HOMO and LUMO energies are scaled in vacuum, redox potentials are generally obtained in solution in the presence of large amounts of an electrolyte. Thus, by using equation (1) electronic reorganization and the differing solvation energies of oxidized and reduced species are disregarded. However, if structurally similar compounds are compared, it can be assumed that solvation and interaction with the electrolyte are comparable and that relative energies are quite accurate within a margin of ca. 0.1 eV.<sup>[36]</sup> Comparing values obtained in different solvents or between solution and the solid state is problematic and unreliable.



**Table 2.** Anodic and cathodic peak potentials<sup>[a]</sup> determined by cyclic voltammetry in acetonitrile and derived HOMO and LUMO energies.<sup>[b]</sup>

| comp.                                    | open isomer         |                |                      |                 | closed isomer  |                |                |                 |                 |
|--|---------------------|----------------|----------------------|-----------------|----------------|----------------|----------------|-----------------|-----------------|
|  | $E_p^{a1} / V$      | $E_p^{c1} / V$ | $E_{HOMO} / eV$      | $E_{LUMO} / eV$ | $E_p^{a1} / V$ | $E_p^{a2} / V$ | $E_p^{c1} / V$ | $E_{HOMO} / eV$ | $E_{LUMO} / eV$ |
| <b>1-CyH<sub>6</sub></b> <sup>[16]</sup> | 1.08                | < -2.80        | -5.88                | -               | 0.24           | 0.53           | -1.84          | -5.04           | -2.96           |
| <b>1-CyF<sub>6</sub></b> <sup>[16]</sup> | 1.79                | -2.40          | -6.59                | -2.40           | 0.76           | -              | -1.27          | -5.56           | -3.53           |
| <b>2-CyH<sub>6</sub></b> <sup>[16]</sup> | 1.06                | -2.38          | -5.86                | -2.42           | 0.61           | 0.88           | -1.61          | -5.41           | -3.19           |
| <b>2-CyF<sub>6</sub></b> <sup>[16]</sup> | 2.00 <sup>[c]</sup> | -2.11          | -6.80 <sup>[c]</sup> | -2.69           | 1.35           | -              | -1.08          | -6.15           | -3.72           |
| <b>2-MI</b>                              | 1.63                | -1.57          | -6.43                | -3.23           | 1.10           | -              | -1.21          | -5.90           | -3.59           |
| <b>3-CH<sub>3</sub></b> <sup>[16]</sup>  | 0.79                | < -2.80        | -5.59                | -               | 0.03           | 0.27           | -2.17          | -4.83           | -2.63           |
| <b>3-CF<sub>3</sub></b>                  | 1.49                | -2.70          | -6.29                | -2.10           | 0.45           | 0.67           | -1.89          | -5.25           | -2.91           |
| <b>4-CH<sub>3</sub></b> <sup>[16]</sup>  | 0.84                | -2.85          | -5.64                | -1.95           | 0.40           | 0.61           | -1.99          | -5.20           | -2.81           |
| <b>4-CF<sub>3</sub></b>                  | 1.52                | -2.39          | -6.32                | -2.41           | 0.88           | 1.03           | -1.70          | -5.68           | -3.10           |
| <b>4-mixed</b>                           | 1.08                | -2.50          | -5.88                | -2.30           | 0.68           | 0.90           | -1.87          | -5.48           | -2.93           |
| <b>5-CH<sub>3</sub></b> <sup>[16]</sup>  | 0.13                | < -2.80        | -4.93                | -               | -0.37          | -              | -2.40          | -4.43           | -2.40           |
| <b>5-CF<sub>3</sub></b>                  | 0.42                | -2.78          | -5.22                | -2.02           | -0.13          | -              | -2.22          | -4.67           | -2.58           |
| <b>6</b> <sup>[16]</sup>                 | 0.22 <sup>[d]</sup> | -2.71          | -5.02                | -2.09           | -0.13          | 0.09           | -2.02          | -4.67           | -2.78           |
| <b>7</b> <sup>[e]</sup>                  | 0.93                | -2.21          | -5.73                | -2.59           | 0.11           | 0.46           | -1.91          | -4.91           | -2.89           |
| <b>8</b>                                 | 0.40 <sup>[f]</sup> | < -2.80        | -5.20                | -               | 0.01           | -              | -2.23          | -4.81           | -2.57           |

[a] All values are reported against the ferrocene/ferrocenium redox couple used as external standard. [b]  $E_{HOMO/LUMO} = -e \cdot E_p^{a1/c1} - 4.8$  eV. [c] Approximate value due to overlapping onset of solvent oxidation. [d]  $E_p^{a2} = 0.64$  V. [e] In methylene chloride. [f]  $E_p^{a2} = 0.95$  V.

2) Generally, the half-wave potential of a fully reversible peak is taken as a measure for the formal potential of the redox process. However, in case of DAEs also irreversible processes are observed, in particular for oxidation of the open isomers. Therefore, we report peak potentials for *all* observed redox waves. In case of fully reversible processes the difference between the half-wave potential and the peak potential amounts to 29 mV and can be neglected. For irreversible processes, which are due to a chemical reaction following the electron transfer, e.g. ring-closure for some ring-open DAEs, the observed peak potential is shifted to lower values compared to the formal potential of the electron transfer. This shift can amount up to approximately 350 mV for very fast chemical reactions. However, for slower reactions the shift is smaller and in case of quasireversible processes it can be neglected. Thus, HOMO and LUMO levels of open isomers showing fully irreversible redox processes have to be treated with care. In contrast, redox processes of most closed isomers are reversible or quasireversible and hence HOMO and LUMO levels can be regarded as more reliable.

3) The offset of 4.8 eV relating the ferrocene/ferrocenium redox couple to the vacuum scale is under debate and a number of different conversion scales with values between 4.5 - 5.4 eV

exist in the literature.<sup>[36]</sup> Therefore, care has to be taken which conversion scale is applied when comparing to literature data.

Though these arguments make the utilization of cyclic voltammetry for the estimation of frontier orbital energies appear rather unreliable, the procedure often is successfully applied for the prediction of specific device properties in the field of organic electronics.<sup>[37]</sup> The method is an easy, cheap, and fast way to select derivatives that fulfill specific energetic requirements out of a collection of compounds. Thereby, for the reasons stated above, comparing *relative* energies of structurally similar derivatives is much more precise than their positioning on an *absolute* scale. Note that in the literature<sup>[38]</sup> correlations between HOMO energies found by cyclic voltammetry with values determined by ultraviolet photoelectron spectroscopy (UPS) generally show a linear dependence even for structurally very different compounds, though the slope may slightly deviate from unity.<sup>[39]</sup>

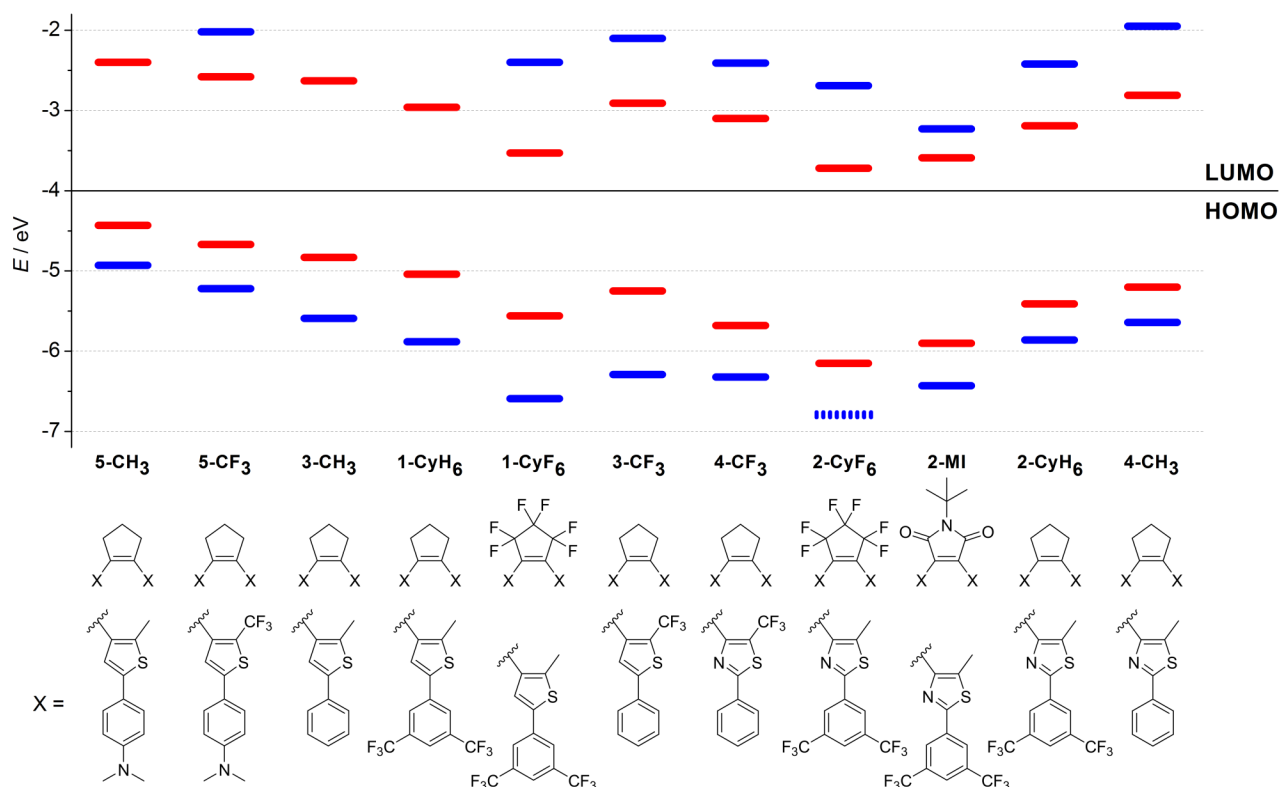


**Figure 6.** Tuning of HOMO and LUMO energies, as obtained from oxidation and reduction potentials by cyclovoltammetry, via donor and acceptor substitution of symmetrical DAEs in their open (blue) and closed (red) form. The bridging unit as well as the heterocyclic building blocks for each compound are depicted below. For compound **2-CyF<sub>6</sub>** the oxidation potential of the open isomer is in the range of the onset of solvent oxidation, thus only an approximate value can be given, indicated by a dashed line.

Electrochemical data of all investigated compounds can be found in Table 2 and in Section 2 of the Supporting Information. Derived HOMO and LUMO levels of symmetrically substituted DAEs are collected in Figure 6, giving an overview over the covered range of absolute frontier orbital energies and the extent of their modulation by the photoisomerization process. A similar representation, also including some other DAE derivatives reported earlier by us,<sup>[15b,16,17,19]</sup> is shown in Figure S21 of the Supporting Information. From these data the following general trends can be derived:

- Absolute energies of the frontier molecular orbitals can be systematically tuned over a broad range covering more than 2.4 eV for HOMO levels (**5-CH<sub>3</sub>** vs. **2-CyF<sub>6</sub>**) and at least 1.8 eV for LUMO levels (**4-CH<sub>3</sub>** vs. **2-CyF<sub>6</sub>**). Note that LUMO levels of most open dithienylethenes are expected to be positioned above -1.9 eV, the limit of accessible potentials in the CV experiments.
- The variation of the substituent in the periphery from strongly donating (4-Me<sub>2</sub>N in **5-CH<sub>3</sub>**) to strongly accepting (3,5-(CF<sub>3</sub>)<sub>2</sub> in **1-CyH<sub>6</sub>**) shifts HOMO levels of open and closed isomers over a total range of 0.95 eV and 0.61 eV, respectively. By using substituents with an intermediate

donor/acceptor character a precise fine-tuning of the energetic levels can be achieved.

- The nature of the bridging unit has an effect of similar magnitude: Diarylperfluorocyclopentene derivatives possess HOMO and LUMO energies about 0.5–1 eV lower than their perhydrocyclopentene analogues (**1-CyH<sub>6</sub>/2-CyH<sub>6</sub>** vs. **1-CyF<sub>6</sub>/2-CyF<sub>6</sub>**). The electron-withdrawing capability of the *N-tert*-butylmaleimide bridge in the closed isomer is slightly smaller than that of perfluorocyclopentene (**2-MI** vs. **2-CyF<sub>6</sub>**), however, the electron affinity of the open isomer of **2-MI** is strongly increased (and higher than that of **2-CyF<sub>6</sub>**) due to the redox active carbonyl groups present in the bridge.
- Substitution with  $\alpha$ -CF<sub>3</sub> groups has a strong effect on HOMO and LUMO levels of open isomers, as can be seen by comparing DAEs **3-CH<sub>3</sub>** and **3-CF<sub>3</sub>** as well as **4-CH<sub>3</sub>** and **4-CF<sub>3</sub>**, which show shifts between 0.5–0.7 eV. In contrast, the effect on closed isomers is smaller with shifts between 0.3–0.4 eV. The latter can readily be explained by the quaternary carbon atoms, which decouple the CF<sub>3</sub> groups from the  $\pi$ -system in the closed isomers. Thus,  $\alpha$ -

trifluoromethyl substitution significantly increases the relative shifts of energy levels upon ring-closure.

- Further fine-tuning of absolute energy levels can be achieved by exchanging thiophene with thiazole heterocycles in otherwise identical structures. For analogous substitution patterns HOMO and LUMO levels of thiazole derivatives are positioned between 0.1 – 0.5 eV lower in energy than their thiophene counterparts.
- Large relative shifts in HOMO and LUMO levels comparing open and closed isomers are obtained upon increasing acceptor substitution of the DAE scaffold. Thereby, dithienylethenes generally show a larger isomerization induced variation than their thiazole analogues. Maximum relative shifts of more than 1 eV can be achieved using the strongly acceptor substituted DAE **1-CyF<sub>6</sub>** as well as the  $\alpha$ -CF<sub>3</sub> substituted derivative **3-CF<sub>3</sub>**.

All together the variation of substituents, in particular using chemically robust fluorinated groups, either in the periphery, in the bridge, or at the ring-closing carbon atoms represents a versatile toolbox to specifically tailor the electronic properties of DAE derivatives according to the energetic requirements within the desired application. We have successfully applied this toolbox for the construction of light-controllable organic thin film transistors by incorporating specifically selected DAE switches into various small molecule as well as polymeric semiconducting matrices.<sup>15</sup> Thereby, the alignment of the HOMO or LUMO energies of the two isomers of a DAE with respect to that of a p-type or n-type semiconductor allowed for the reversible trapping of holes or electrons within the matrix dependent on the switching state of the DAE. From our work it has become evident that small variations in the relative energy levels between the DAE and the semiconductor directly affect the photoswitching performance of the overall device, illustrating the importance of being able to precisely fine-tune the electronic properties of the photoswitchable charge trap.

In order to rationalize and possibly predict the influence of distinct substitution patterns on the electronic properties of the DAE scaffold we performed DFT calculations and theoretically assessed HOMO and LUMO energies. Thereby we note that theoretically predicted MO energies typically are sensitive to the choice of the functional and size of the basis set and that an empirical correlation to experimental values is only valid for a homologous series of chemical compounds. Comparing the HSEh1PBE<sup>[40]</sup> and B3LYP<sup>[41]</sup> functionals using the 6-311+G(d,p) basis set we found that B3LYP provides a slightly better agreement between experimental and theoretical data. Notably, after implementing the solvent acetonitrile using the polarizable *continuum* model (PCM) the dispersion of theoretical HOMO and LUMO levels around the experimental values was significantly reduced such that we obtained a surprisingly good linear correlation (Figure 7). The slope of the correlation is nearly unity for both HOMO and LUMO energies, whereas there is a slightly different offset for the two data sets. Based on this correlation it is possible to theoretically predict frontier orbital levels of *de novo* designed DAE derivatives with specific electronic properties.

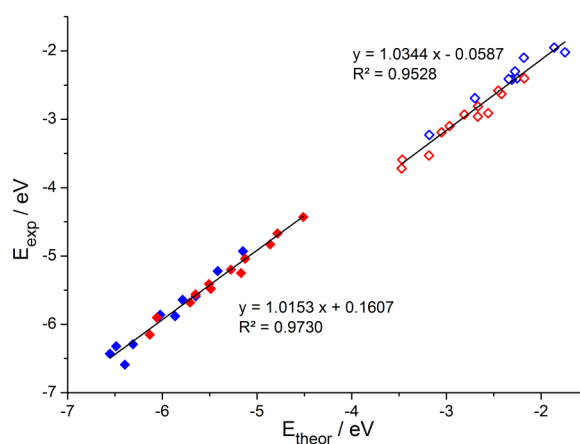


**Figure 7.** Correlation between experimental and theoretical (B3LYP/PCM(acetonitrile)/6-311+G(d,p)) HOMO (filled symbols) and LUMO (empty symbols) energies of open (blue) and closed (red) isomers.

#### Transduction of electronic changes to redox active groups.

In order to have a model on how much of the electronic changes within the DAE core can be transduced to an adjacent functional group nonsymmetrically substituted DAEs **6-8** were designed bearing redox markers and acceptor groups in different configurations (see Figure 2). In terms of modulating the electron density of an *N,N*-dimethylaniline group by the switching process compounds **6** and **8** represent the “mismatched” and “matched” case, respectively, for the coupling with the acceptor group. For both compounds the first oxidation processes are fully reversible in the ring-open and ring-closed forms and can be assumed to be located at the *N,N*-dimethylaniline unit (Figure 8). Note that, similar to symmetrically *N,N*-dimethylaniline substituted compounds **5-CH<sub>3</sub>** and **5-CF<sub>3</sub>**, for the closed isomer of **8** a two-electron oxidation wave is observed. From the difference of the anodic and cathodic peak currents it can be derived that two one-electron oxidation processes with a potential splitting of less than 100 mV are occurring.

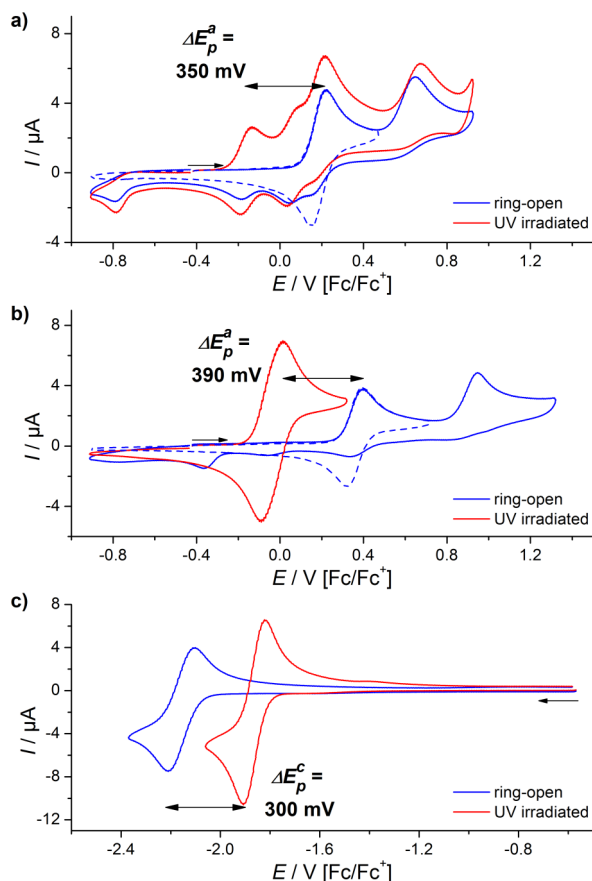


**Figure 8.** Cyclic voltammograms ( $dE/dt = 1 \text{ V s}^{-1}$ ) of DAEs a) **6** in acetonitrile/0.1 M  $\text{Bu}_4\text{NPF}_6$ , b) **8** in acetonitrile/0.1 M  $\text{Bu}_4\text{NPF}_6$ , and c) **7** in methylene chloride/0.1 M  $\text{Bu}_4\text{NPF}_6$ . All concentrations were  $1 \cdot 10^{-3} \text{ M}$  before irradiation. For compound **6** only low conversion to the closed isomer could be achieved after extended irradiation of the electrochemical cell for 2.5 h. Note that for a) and c) solutions became more concentrated during the irradiation procedure due to long irradiation times needed in case of a) and high volatility of the solvent in case of c).

The potential of the first oxidation process of the open isomer of **8** is higher by 180 mV when compared to **6** and by 270 mV when compared to **5-CH<sub>3</sub>**, which is in accordance with the expectation that the  $\text{CF}_3$  group in the  $\alpha$ -position of the thiophene ring would decrease the electron density of the aniline moiety (Figure 2). A very similar potential is observed for the symmetrically substituted analogue **5-CF<sub>3</sub>** showing that the two termini of the DAE are electronically isolated in the ring-open form. Given the much larger electronic effect of  $\alpha$ - $\text{CF}_3$  groups on the electron density within the DAE core itself, observed by comparing compounds **3-CH<sub>3</sub>/4-CH<sub>3</sub>** and **3-CF<sub>3</sub>/4-CF<sub>3</sub>** (*vide supra*), it can already be inferred that transduction of the electronic changes to an adjacent functional unit such as the *N,N*-dimethylaniline moiety is significantly less pronounced. Note that compared to the open isomer of **5-CH<sub>3</sub>** the first oxidation of **6** is shifted by 90 mV to higher potentials, although both compounds are expected to possess the same redox behavior in the first step as in the ring-open form of **6** the acceptor moiety at

the opposite terminus of the DAE should not interfere with the aniline.

In contrast, for the ring-closed isomer of **6**, with the *N,N*-dimethylaniline moiety being coupled to the electron-withdrawing 3,5-bis(trifluoromethyl)phenyl group, it was expected that its first oxidation would appear at higher potentials than the first oxidation of the closed isomer of **8**, for which the  $\pi$ -electronic system is decoupled from the  $\alpha$ - $\text{CF}_3$  group. Instead, it is experimentally found that the oxidation of the closed isomer of **6** at  $E_p^{at} = -0.13 \text{ V}$  occurs at a slightly lower potential than that of **8** at  $E_p^{at} = 0.01 \text{ V}$ . This shows that in the closed form the effect of the acceptor group at the opposite terminus through the conjugated DAE core is rather limited while the  $\text{CF}_3$  group in  $\alpha$  position of the heteraryl ring still has a significant impact on the  $\pi$ -electronic system, though it is separated by an additional  $\text{sp}^3$ -carbon. As a result, the difference between the two DAE derivatives **6** and **8** in their relative potential shift upon ring-closure is small. Though the shift is slightly larger in the "matched" compound **8** with a value of 390 mV, the shift of 350 mV for the "mismatched" compound **6** is comparable.

A similar potential shift of 300 mV between the open and closed isomers is observed for the reversible reduction of DAE **7** which is located at the triphenyltriazine moiety. As this compound already represents the "matched" case, the synthesis of the "mismatched" analogue was not attempted.

## Conclusions

In this work we demonstrate that the HOMO and LUMO energies of DAE photoswitches can be precisely tuned over a broad range by donor/acceptor substitution in the periphery, variation of the bridging moiety, substitution with  $\text{CF}_3$  groups in the  $\alpha$ -positions of the heteraryl rings, and exchange of thiophene with thiazole heterocycles. Some of these derivatives exhibit remarkable photoisomerization induced shifts of the energies of their frontier molecular orbital energy levels of more than 1 eV. By creating a large collection of electronically modulated DAEs, by estimating the effects of structural modifications, and by establishing a theoretical model based on correlating experimental and computational data it is now possible to custom-design specific DAE derivatives that fulfill energetic requirements for potential applications, in particular in combination with other (opto)electronically active materials to reversibly enable and disable charge transport (or energy transfer) between the building blocks. In the future we will be able to use this insight to screen the electronic properties of hitherto unknown DAE derivatives *in silico* and focus the synthetic efforts only on the most promising candidates.

In contrast to the large electronic modulation induced within the DAE core upon photoisomerization, transduction of these intrinsic changes to an adjacent,  $\pi$ -conjugated functional unit is less pronounced. For model compounds possessing aniline or triazine redox moieties potential shifts between 300 – 400 mV were observed upon ring-closure. Thereby, different patterns of substitution, involving acceptor groups with either "matched" or "mismatched" effects on the  $\pi$ -electronic system of the DAE,



turned out to have only a small influence. In light of the desired property changes of functional units attached to DAEs, such as binding motifs or catalytically active moieties, a larger modulation of electron density is certainly desired. Therefore, the electronic communication between the functional unit and the DAE core should be increased by moving the functional unit closer to the DAE core, for example omitting the phenyl group, or perhaps more promising by using the functional unit itself instead of one thiophene or thiazole heterocycle. Furthermore, electronic modulation can potentially be increased using -M substituents instead of CF<sub>3</sub> groups or by placing the acceptor group at the free  $\beta$ -position of the thiophene ring. Research into these directions is currently ongoing in our laboratories.

In addition to the remarkable electronic properties of  $\alpha$ -trifluoromethylated DAEs, interesting insights into their photochemistry were obtained. DAEs symmetrically substituted with  $\alpha$ -CF<sub>3</sub> groups on both hetaryl rings show a strong reduction of the cyclization quantum yield, whereas the ring-opening quantum yield was significantly increased when compared to the methyl substituted derivatives. Importantly, installing only one CF<sub>3</sub> group on one hetaryl ring restores the usual photochemical behavior of DAEs. The combination of a 4-*N,N*-dimethylaniline donor and a CF<sub>3</sub> acceptor placed in the two  $\alpha$ -positions of one thiophene moiety provides attractive new DAE derivatives, which exhibit a marked bathochromic shift of the absorbance of the open isomer, an increased quantum yield for ring-closure, and good fatigue resistance.

## Acknowledgements

The authors thank Dr. Beatrice Braun-Cula for obtaining single crystal X-ray structural data and Jana Hildebrandt for synthetic support. F.E. thanks the Fonds der Chemischen Industrie for providing a doctoral fellowship. Generous support by the European Research Council (ERC via ERC-2012-STG\_308117 "Light4Function"), the European Commission (via MSCA-ITN "iSwitch" GA No. 642196), and the German Research Foundation (DFG via SFB 658, project B8) is gratefully acknowledged.

**Keywords:** photochromism • diarylethenes • frontier molecular orbital energies • quantum yields • cyclic voltammetry

- [1] a) *Photochromism: Molecules and Systems* (Eds.: H. Dürr, H. Bouas-Laurent), Elsevier Science, Amsterdam, **2003**; b) *Molecular Switches* (Eds.: B. L. Feringa, W. R. Browne), 2nd ed., Wiley-VCH, Weinheim, **2011**; c) *New Frontiers in Photochromism* (Eds.: M. Irie, Y. Yokoyama, T. Seki), Springer Japan, Tokyo, **2013**; d) *Photochromic Materials: Preparation, Properties and Applications* (Eds.: H. Tian, J. Zhang), 1st ed., Wiley-VCH, Weinheim, **2016**.
- [2] a) W.A. Velema, W. Szymanski, B.L. Feringa, *J. Am. Chem. Soc.* **2014**, *136*, 2178-2191; b) J. Broichhagen, J.A. Frank, D. Trauner, *Acc. Chem. Res.* **2015**, *48*, 1947-1960; c) M.M. Lerch, M.J. Hansen, G.M. van Dam, W. Szymanski, B.L. Feringa, *Angew. Chem. Int. Ed.* **2016**, *55*, 10978-10999.
- [3] J.M. Abendroth, O.S. Bushuyev, P.S. Weiss, C.J. Barrett, *ACS Nano* **2015**, *9*, 7746-7768.
- [4] E. Orgiu, P. Samori, *Adv. Mater.* **2014**, *26*, 1827-1845.
- [5] a) M. Irie, T. Fukaminato, K. Matsuda, S. Kobatake, *Chem. Rev.* **2014**, *114*, 12174-12277; b) M. Irie, *Pure Appl. Chem.* **2015**, *87*, 617-626.
- [6] H.D. Samachetty, N.R. Branda, *Pure Appl. Chem.* **2006**, *78*, 2351-2359.
- [7] a) S. Kobatake, S. Takami, H. Muto, T. Ishikawa, M. Irie, *Nature* **2007**, *446*, 778-781; b) F. Terao, M. Morimoto, M. Irie, *Angew. Chem. Int. Ed.* **2012**, *51*, 901-904; c) D. Kitagawa, H. Nishi, S. Kobatake, *Angew. Chem. Int. Ed.* **2013**, *52*, 9320-9322; d) S. Ohshima, M. Morimoto, M. Irie, *Chem. Sci.* **2015**, *6*, 5746-5752.
- [8] a) T. Hirose, M. Irie, K. Matsuda, *Adv. Mater.* **2008**, *20*, 2137-2141; b) J. Kämbart, M. Hammarson, S. Li, H.L. Anderson, B. Albinsson, J. Andréasson, *Angew. Chem. Int. Ed.* **2010**, *49*, 1854-1857; c) S. Yagai, K. Iwai, M. Yamauchi, T. Karatsu, A. Kitamura, S. Uemura, M. Morimoto, H. Wang, F. Würthner, *Angew. Chem. Int. Ed.* **2014**, *53*, 2602-2606; d) M. Han, Y. Luo, B. Damaschke, L. Gómez, X. Ribas, A. Jose, P. Peretzi, M. Seibt, G.H. Clever, *Angew. Chem. Int. Ed.* **2016**, *55*, 445-449.
- [9] a) D. Vomasta, C. Högner, N.R. Branda, B. König, *Angew. Chem. Int. Ed.* **2008**, *47*, 7644-7647; b) C. Falencyk, M. Schiedel, B. Karaman, T. Rumpf, N. Kuzmanovic, M. Grotli, W. Sippl, M. Jung, B. König, *Chem. Sci.* **2014**, *5*, 4794-4799; c) B. Reisinger, N. Kuzmanovic, P. Löffler, R. Merkl, B. König, R. Sterner, *Angew. Chem. Int. Ed.* **2014**, *53*, 595-598; d) O. Babii, S. Afonin, L.V. Garmanchuk, V.V. Nikulina, T.V. Nikolaienko, O.V. Storozhuk, D.V. Shelest, O.I. Dasyukevich, L.I. Ostapchenko, V. Iurchenko, S. Zozulya, A.S. Ulrich, I.V. Komarov, *Angew. Chem. Int. Ed.* **2016**, *55*, 5493-5496.
- [10] a) T. Fukaminato, T. Sasaki, T. Kawai, N. Tamai, M. Irie, *J. Am. Chem. Soc.* **2004**, *126*, 14843-14849; b) T. Fukaminato, T. Doi, N. Tamaoki, K. Okuno, Y. Ishibashi, H. Miyasaka, M. Irie, *J. Am. Chem. Soc.* **2011**, *133*, 4984-4990; c) T. Fukaminato, *J. Photochem. Photobiol., C* **2011**, *12*, 177-208; d) M. Pärs, C.C. Hofmann, K. Willinger, P. Bauer, M. Thelakktat, J. Köhler, *Angew. Chem. Int. Ed.* **2011**, *50*, 11405-11408; e) M. Berberich, M. Natali, P. Spenst, C. Chiorboli, F. Scandola, F. Würthner, *Chem. Eur. J.* **2012**, *18*, 13651-13664.
- [11] L. Hou, X. Zhang, T.C. Pijper, W.R. Browne, B.L. Feringa, *J. Am. Chem. Soc.* **2014**, *136*, 910-913.
- [12] K. Xu, J. Zhao, X. Cui, J. Ma, *Chem. Commun.* **2015**, *51*, 1803-1806.
- [13] a) N. Katsonis, T. Kudernac, M. Walko, S.J. van der Molen, B.J. van Wees, B.L. Feringa, *Adv. Mater.* **2006**, *18*, 1397-1400; b) C. Jia, J. Wang, C. Yao, Y. Cao, Y. Zhong, Z. Liu, Z. Liu, X. Guo, *Angew. Chem. Int. Ed.* **2013**, *52*, 8666-8670; c) F. Meng, Y.-M. Hervault, Q. Shao, B. Hu, L. Norel, S. Rigaut, X. Chen, *Nat. Commun.* **2014**, *5*, 3023; d) T. Toyama, K. Higashiguchi, T. Nakamura, H. Yamaguchi, E. Kusaka, K. Matsuda, *J. Phys. Chem. Lett.* **2016**, *7*, 2113-2118; e) C. Jia, A. Migliore, N. Xin, S. Huang, J. Wang, Q. Yang, S. Wang, H. Chen, D. Wang, B. Feng, Z. Liu, G. Zhang, D.-H. Qu, H. Tian, M.A. Ratner, H.Q. Xu, A. Nitzan, X. Guo, *Science* **2016**, *352*, 1443-1445.
- [14] a) A.J. Kronemeijer, H.B. Akkerman, T. Kudernac, B.J. van Wees, B.L. Feringa, P.W.M. Blom, B. de Boer, *Adv. Mater.* **2008**, *20*, 1467-1473; b) P. Zacharias, M.C. Gather, A. Köhnen, N. Rehmman, K. Meerholz, *Angew. Chem. Int. Ed.* **2009**, *48*, 4038-4041; c) R.C. Shallcross, P.O. Körner, E. Maibach, A. Köhnen, K. Meerholz, *Adv. Mater.* **2013**, *25*, 4807-4813; d) R. Hayakawa, K. Higashiguchi, K. Matsuda, T. Chikyo, Y. Wakayama, *ACS Appl. Mater. Interfaces* **2013**, *5*, 3625-3630.
- [15] a) E. Orgiu, N. Crivillers, M. Herder, L. Grubert, M. Pätzl, J. Frisch, E. Pavlica, D.T. Duong, G. Bratina, A. Salleo, N. Koch, S. Hecht, P. Samori, *Nature Chem.* **2012**, *4*, 675-679; b) M.E. Gemayel, K. Börjesson, M. Herder, D.T. Duong, J.A. Hutchison, C. Ruzié, G. Schweicher, A. Salleo, Y. Geerts, S. Hecht, E. Orgiu, P. Samori, *Nat. Commun.* **2015**, *6*, 6330; c) K. Börjesson, M. Herder, L. Grubert, D.T. Duong, A. Salleo, S. Hecht, E. Orgiu, P. Samori, *J. Mater. Chem. C* **2015**, *3*, 4156-4161; d) T. Leydecker, M. Herder, E. Pavlica, G. Bratina, S. Hecht, E. Orgiu, P. Samori, *Nat. Nanotechnol.* **2016**, *11*, 769-775.

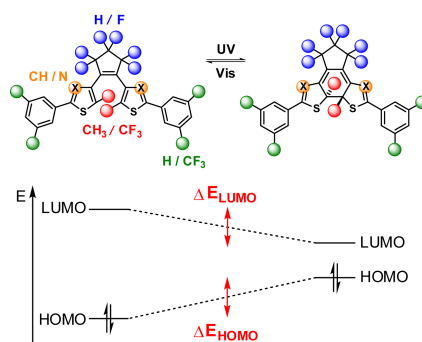


- [16] M. Herder, B.M. Schmidt, L. Grubert, M. Pätzelt, J. Schwarz, S. Hecht, *J. Am. Chem. Soc.* **2015**, *137*, 2738-2747.
- [17] M. Herder, M. Utecht, N. Manicke, L. Grubert, M. Pätzelt, P. Saalfrank, S. Hecht, *Chem. Sci.* **2013**, *4*, 1028-1040.
- [18] For examples demonstrating the photomodulation of the electronic properties of a chemically reactive site in the bridge of a DAE see: a) V. Lemieux, M. Spantulescu, K. Baldrige, N. Branda, *Angew. Chem. Int. Ed.* **2008**, *47*, 5034-5037; b) T. Nakashima, M. Goto, S. Kawai, T. Kawai, *J. Am. Chem. Soc.* **2008**, *130*, 14570-14575; c) A.J. Teator, Y. Tian, M. Chen, J.K. Lee, C.W. Bielawski, *Angew. Chem. Int. Ed.* **2015**, *54*, 11559-11563; d) B. Rösner, M. Milek, A. Witt, B. Gobaut, P. Torelli, R.H. Fink, M.M. Khusniyarov, *Angew. Chem. Int. Ed.* **2015**, *54*, 12976-12980. For examples in the periphery of a DAE see: e) S.H. Kawai, S.L. Gilat, J.-M. Lehn, *Eur. J. Org. Chem.* **1999**, *1999*, 2359-2366; f) Y. Odo, K. Matsuda, M. Irie, *Chem. Eur. J.* **2006**, *12*, 4283-4288; g) H.D. Samachetty, V. Lemieux, N.R. Branda, *Tetrahedron* **2008**, *64*, 8292-8300; h) M. Morimoto, K. Murata, T. Michinobu, *Chem. Commun.* **2011**, *47*, 9819-9821; i) D. Wilson, N.R. Branda, *Angew. Chem.* **2012**, *124*, 5527-5530; j) G. Bianchini, G. Strukul, D.F. Wass, A. Scarso, *RSC Adv.* **2015**, *5*, 10795-10798; k) M. Kathan, P. Kovaříček, C. Jurissek, A. Senf, A. Dallmann, A.F. Thünemann, S. Hecht, *Angew. Chem. Int. Ed.* **2016**, *55*, 13882-13886.
- [19] M. Herder, M. Pätzelt, L. Grubert, S. Hecht, *Chem. Commun.* **2011**, *47*, 460-462.
- [20] S. Hiroto, K. Suzuki, H. Kamiya, H. Shinokubo, *Chem. Commun.* **2011**, *47*, 7149-7151.
- [21] J.J.D. de Jong, L.N. Lucas, R. Hania, A. Pugzlys, R.M. Kellogg, B.L. Feringa, K. Duppen, J.H. van Esch, *Eur. J. Org. Chem.* **2003**, *2003*, 1887-1893.
- [22] H. Urata, T. Fuchikami, *Tetrahedron Lett.* **1991**, *32*, 91-94.
- [23] H. Morimoto, T. Tsubogo, N.D. Litvinas, J.F. Hartwig, *Angew. Chem. Int. Ed.* **2011**, *50*, 3793-3798.
- [24] M. Holzweber, M. Schnürch, P. Stanetty, *Synlett* **2007**, *2007*, 3016-3018.
- [25] M. Ohsumi, M. Hazama, T. Fukaminato, M. Irie, *Chem. Commun.* **2008**, 3281-3283.
- [26] a) M. Irie, T. Eriguchi, T. Takada, K. Uchida, *Tetrahedron* **1997**, *53*, 12263-12271; b) A. Thomas Bens, D. Frewert, K. Kodatis, C. Krysch, H.-D. Martin, H.P. Trommsdorff, *Eur. J. Org. Chem.* **1998**, *1998*, 2333-2338.
- [27] a) K. Morimitsu, S. Kobatake, S. Nakamura, M. Irie, *Chem. Lett.* **2003**, *32*, 858-859. The contrary effect is observed in case of +M substituents at the alpha carbons: b) K. Shibata, S. Kobatake, M. Irie, *Chem. Lett.* **2001**, *30*, 618-619; c) S. Takami, T. Kawai, M. Irie, *Eur. J. Org. Chem.* **2002**, *2002*, 3796-3800; d) K. Higashiguchi, K. Matsuda, Y. Asano, A. Murakami, S. Nakamura, M. Irie, *Eur. J. Org. Chem.* **2005**, *2005*, 91-97.
- [28] a) K. Uchida, E. Tsuchida, Y. Aoi, S. Nakamura, M. Irie, *Chem. Lett.* **1999**, *28*, 63-64; b) W. Li, C. Jiao, X. Li, Y. Xie, K. Nakatani, H. Tian, W. Zhu, *Angew. Chem. Int. Ed.* **2014**, *53*, 4603-4607.
- [29] A. Fihey, D. Jacquemin, *Chem. Sci.* **2015**, *6*, 3495-3504.
- [30] a) M. Irie, K. Sayo, *J. Phys. Chem.* **1992**, *96*, 7671-7674; b) M. Irie, K. Sakemura, M. Okinaka, K. Uchida, *J. Org. Chem.* **1995**, *60*, 8305-8309.
- [31] M. Irie, T. Lifka, K. Uchida, S. Kobatake, Y. Shindo, *Chem. Commun.* **1999**, 747-750.
- [32] CCDC-1518489 contains the supplementary crystallographic data for this paper. These data can be obtained free of charge from [The Cambridge Crystallographic Data Centre](http://www.ccdc.cam.ac.uk).
- [33] a) P.D. Patel, I.A. Mikhailov, K.D. Belfield, A.E. Masunov, *Int. J. Quantum Chem.* **2009**, *109*, 3711-3722; b) D. Mendive-Tapia, A. Perrier, M.J. Bearpark, M.A. Robb, B. Lasorne, D. Jacquemin, *Phys. Chem. Chem. Phys.* **2014**, *16*, 18463-18471; c) J.R. Matis, J.B. Schonborn, P. Saalfrank, *Phys. Chem. Chem. Phys.* **2015**, *17*, 14088-14095.
- [34] I. Fernández, F.P. Cossio, M.A. Sierra, *Chem. Rev.* **2009**, *109*, 6687-6711.
- [35] J. Pommerehne, H. Vestweber, W. Guss, R.F. Mahrt, H. Bässler, M. Porsch, J. Daub, *Adv. Mater.* **1995**, *7*, 551-554.
- [36] C.M. Cardona, W. Li, A.E. Kaifer, D. Stockdale, G.C. Bazan, *Adv. Mater.* **2011**, *23*, 2367-2371.
- [37] Y. Shiota, H. Kageyama, *Chem. Rev.* **2007**, *107*, 953-1010.
- [38] a) B.W. D'Andrade, S. Datta, S.R. Forrest, P. Djurovich, E. Polikarpov, M.E. Thompson, *Org. Electron.* **2005**, *6*, 11-20; b) P. Zacharias, M.C. Gather, M. Rojahn, O. Nuyken, K. Meerholz, *Angew. Chem. Int. Ed.* **2007**, *46*, 4388-4392.
- [39] In our hands relative HOMO energies of two DAE derivatives determined by UPS measurements were similar to cyclic voltammetric data. However, absolute values slightly differed between the two methods. See reference [15a] as well as: J. Frisch, M. Herder, P. Herrmann, G. Heimel, S. Hecht, N. Koch, *Appl. Phys. A* **2013**, *113*, 1-4.
- [40] J. Heyd, G.E. Scuseria, *J. Chem. Phys.* **2004**, *121*, 1187-1192.
- [41] a) A.D. Becke, *J. Chem. Phys.* **1993**, *98*, 5648-5652; b) P.J. Stephens, F.J. Devlin, C.F. Chabalowski, M.J. Frisch, *J. Phys. Chem.* **1994**, *98*, 11623-11627.

## Entry for the Table of Contents

## FULL PAPER

**Photocontrol over energy levels:** By decorating photochromic diarylethenes with fluorinated substituents HOMO and LUMO energy levels of both isomers are precisely tuned over a broad range and the effect of the switching event is maximized. The light-induced electronic shifts can be transduced to adjacent functional groups in order to modulate their properties.



*Martin Herder, Fabian Eisenreich, Aurelio Bonasera, Anna Grafl, Lutz Grubert, Michael Pätzel, Jutta Schwarz, and Stefan Hecht\**

**Page No. – Page No.**

**Light-Controlled Reversible Modulation of Frontier Molecular Orbital Energy Levels in Trifluoromethylated Diarylethenes**